

RSC Advances

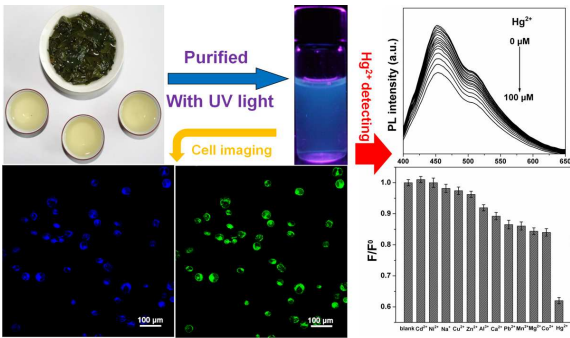


This is an *Accepted Manuscript*, which has been through the Royal Society of Chemistry peer review process and has been accepted for publication.

Accepted Manuscripts are published online shortly after acceptance, before technical editing, formatting and proof reading. Using this free service, authors can make their results available to the community, in citable form, before we publish the edited article. This *Accepted Manuscript* will be replaced by the edited, formatted and paginated article as soon as this is available.

You can find more information about *Accepted Manuscripts* in the [Information for Authors](#).

Please note that technical editing may introduce minor changes to the text and/or graphics, which may alter content. The journal's standard [Terms & Conditions](#) and the [Ethical guidelines](#) still apply. In no event shall the Royal Society of Chemistry be held responsible for any errors or omissions in this *Accepted Manuscript* or any consequences arising from the use of any information it contains.



Water-soluble, highly photoluminescent carbonaceous nanodots were obtained from tea water and were applied to Hg²⁺ detecting and cell imaging.

Cite this: DOI: 10.1039/c0xx00000x

www.rsc.org/xxxxxx

ARTICLE TYPE

Dual Functional Carbonaceous Nanodots Exist in a Cup of Tea

Jumeng Wei^{a,†}, Bitao Liu^{b,*‡}, Peng Yin^c

Received (in XXX, XXX) Xth XXXXXXXXX 20XX, Accepted Xth XXXXXXXXX 20XX

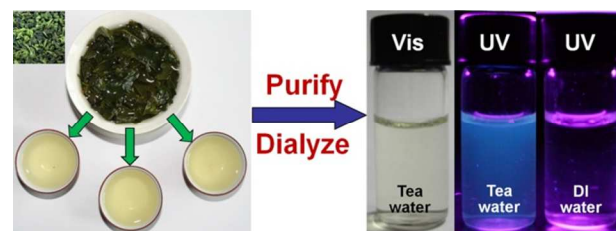
DOI: 10.1039/b000000x

Abstract: Highly photoluminescent (PL) carbonaceous nanodots (CNDs) with a PL quantum yield (PLQY) of 6.8% have been discovered and obtained from tea water. The characterizations indicated that the CNDs show amorphous structure, good monodispersity, excellent water-solubility, interesting PL properties, acceptable PL lifetime, fairly good photostability and biocompatibility, which can enable the obtained CNDs to be applied to Hg²⁺ detecting and cell imaging.

1. Introduction

Carbon is one of the most common elements in nature, and abundant in the atmosphere and crust in a variety of forms. For centuries, carbon has been known as a macroscopic, black material. While recently, a variety of carbon materials with remarkable physical and chemical properties were developed, fullerene,^{1,2} carbon nanotubes,³ graphene,⁴ and CNDs.⁵⁻⁷ Among such discoveries, photoluminescent CNDs are attracting more and more interests due to their small particle size, excitation wavelength dependent behavior, non-blinking photoluminescence emission, and favourable biocompatibility, potential applications in heavy metal ions detection,⁸⁻¹⁰ biological labeling,^{11,12} optical sensor,¹³ optoelectronic devices,¹⁴ and photocatalysis.¹⁵⁻¹⁷ To date, methods that have been developed to prepare photoluminescent CNDs include laser ablation,¹⁸ microwave-assist,^{19,20} electrochemical oxidation,²¹ arc-discharge,²² and acid dehydration.²³ However, these approaches usually involve complex reactions and post-treatment processes, and expensive carbon source. Thus, the practical applications of CNDs have been severely limited.

Lately, several unprecedented scientific researchers have demonstrated new simple synthetic pathways of carbonaceous nanomaterials. The Mohapatra's group and Dong *et al.* prepared high-quality, photoluminescent, functional CNDs from orange juice and soy milk, respectively.^{24,25} Inspired by these works, our group has been working on finding simpler, milder methods to prepare photoluminescent CNDs using renewable biomass as carbon source. On one occasion, we found that a glass of tea water showed blue photoluminescence upon exposure to UV light. Subsequent to this discovery, we investigated the tea water by means of abundant characterizations and testings. These investigations demonstrate that water-soluble and highly photoluminescent CNDs exist in the tea water. The applications of tea in material science have, to the best of our knowledge, not yet been reported, despite being used as a beverage for thousands of years. The unique photoluminescence properties and fairly good biocompatibility can enable the as-prepared CNDs to be



Scheme 1 Illustration of the preparation procedure of the CNDs (photograph of the samples excited by daylight and a 365 UV lamp).

applied to Hg²⁺ detecting and cell imaging.

2. Experimental sections

2.1. The preparation of photoluminescent CNDs.

The synthesis procedure is shown in Scheme 1. Briefly, 3 g dry tea leaves (Tieguanyin, China) infused in 200 ml boiling deionized (DI) water (about 100 °C), and 20 minutes later a cup of tea was obtained (Scheme 1). The faint yellow tea water was centrifuged at high speed (22000 rpm) to separate the precipitate. Subsequently, excess methylbenzene was added into the tea water to extract the organics (eg. protein, polycyclic aromatic hydrocarbon (PAH)), the mixture was shaken for 30 minutes, and the upper solution containing CNDs was collected after 1 hour standing. Finally, the CNDs solution was dialyzed against DI water for two days by dialysis membrane (molecular weight cut-off (MWCO): 3500) to remove almost all of impurity inorganic ions and molecules, and the clear and transparent CNDs solution without any precipitation was obtained (Scheme 1). Furthermore, the prepared solution was still clear and transparent even though it was exposed to the open air for several months. The CNDs solution shows light green color under daylight and changes to a blue color on exposure of 365 nm UV lights (Scheme 1). These observations imply that the resultant CNDs possess fairly good water solubility and photoluminescence.

2.2. Characterizations

UV-Vis absorbance spectroscopic (Abs) studies were performed with a TU-1901 dual beam UV-Vis spectrophotometer. PL

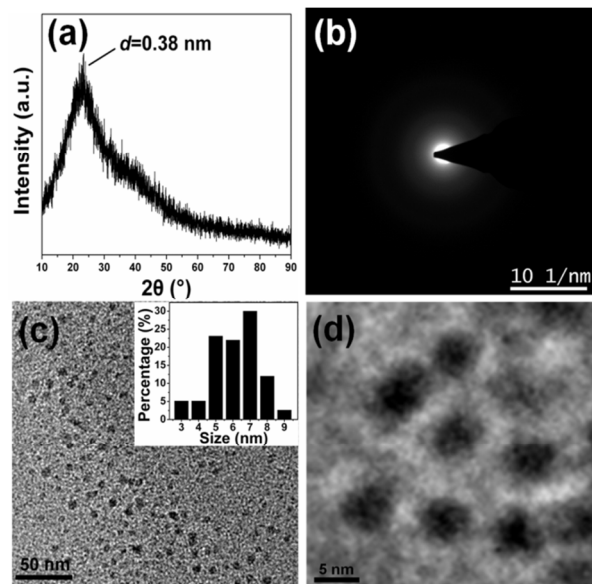


Fig. 1 (a) XRD pattern, (b) SAED pattern, (c) TEM and (d) HRTEM images of the CNDs, (inset: size distribution histogram).

measurements were performed with FLs-920 steady-state/transient-state spectroscopy. The Mn element is determined by means of inductively coupled plasma mass spectrometry (ICP-MS, TJA, IRIS ER/S). The structure of the CNDs was characterized by X-ray diffraction (XRD, Rigaku D/Max-2400) using Cu K α radiation (40 kV, 60 mA). Transmission electron microscopy (TEM), high-resolution TEM (HRTEM) images and selected area electron diffraction (SAED) were acquired by using a Tecnai-G² F30 TEM operating at an acceleration voltage of 300 kV. X-ray photoelectron spectroscopy (XPS) analysis was carried out on ESCALAB 250Xi photoelectron spectrometer. The Fourier transform infrared spectroscopy (FTIR) spectra were measured by a Thermo Nicolet Nexus FTIR model 670 spectrometer. The cellular image was obtained with a laser scanning confocal microscope (LSCM, LSM 510 Meta).

2.3. In vitro cytotoxicity study and cell imaging.

Cytotoxicity study: The cytotoxicity of CNDs was assessed by using the MTT assay. L02 human hepatocyte cells (or S180 sarcoma cells) (1×10^4 cells/well) were grown at 37 °C and under 5% CO₂ atmosphere in RPMI-1640 medium in a 96-well plate, supplemented with calf serum (10%) and 1% penicillin streptomycin in a fully humidified incubator. Then, the CNDs solutions with a concentration of 30, 60, 120, 240, 480 and 960 μ g/mL were added to cell dishes, respectively, and then these cell dishes were put into incubators at 37 °C for 12 h. After incubation for a defined time, the culture medium was removed and 20 μ L of MTT reagent (diluted in culture medium, 0.5 mg/mL) was added, followed by incubating for another 2 h. The MTT/medium was removed carefully and DMSO (150 μ L) was added to each well to dissolve the formazan crystals. Absorbance of the colored solution was measured at 570 nm using a microplate reader.

Cell imaging: After confirming the photoluminescence from CNDs and no distinct auto-photoluminescence from the cell itself under similar conditions, the cellular image was obtained with a laser scanning confocal microscope (LSCM, ZEISS, LSM 510

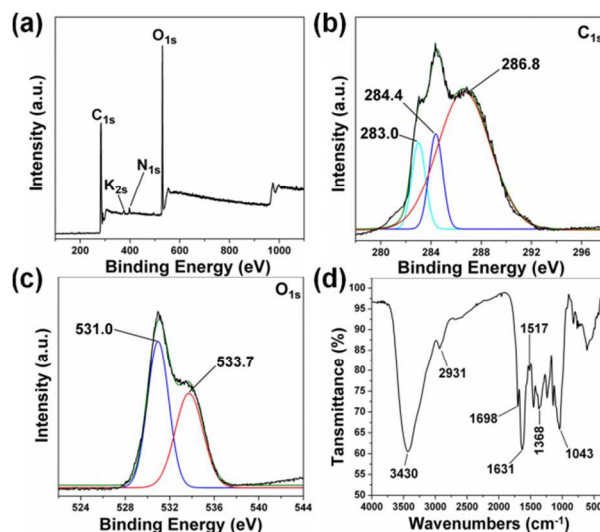


Fig. 2 (a) XPS, (b) C_{1s} and (c) O_{1s} of the CNDs, (d) FTIR spectrum of the CNDs.

Meta, Germany). S180 sarcoma cells (6×10^4 cells/well) were seeded on a 6-well plate at 37 °C for 24 h. After that, the CNDs solution with a concentration of 3 mg/mL was added to the cell dishes. After further 2 h incubation, these CNDs-loaded cells were washed with PBS three times to remove the free CNDs attached on the outer surface of cell membrane. Cell luminescence imaging was detected on LSCM under excitation wavelength of 364 nm and 488 nm.

3. Results and discussion

Fig. 1a presents a typical powder XRD profile of the obtained CNDs. A broad peak centered at $2\theta = 23.4^\circ$ indicates the poor crystalline nature of CNDs, which can be attributed to the amorphous carbon composed in a considerably random fashion.^{26,27} The corresponding interlayer spacing of CNDs ($d = 0.38$ nm) is larger than that of graphite ($d = 0.33$ nm), indicating the CNDs are not graphitic carbon.²⁸ The typical annular SAED (Fig. 1b) also demonstrates the amorphous structure of the obtained CNDs. The TEM image is shown in Fig. 1c, it is found that the CNDs show highly uniform quasi-spherical morphology and fairly good monodispersity. As shown in Fig. 1d, the absence of any discernible lattice structures from the HRTEM image also suggests an amorphous nature of the obtained CNDs, which agrees well with the XRD analysis. Inset of Fig. 1c shows the particle size distribution histogram, which indicates that these quasi-spherical particles are mainly distributed in the range of 3–9 nm (6.8 nm average diameter). The particle size of the obtained CNDs from tea water is similar to that of the CNDs reported previously.^{29,30}

The component and surface states of CNDs were characterized by XPS and FTIR. The wide scan of XPS is shown in Fig. 2a, which reveals that the obtained CNDs contain mainly carbon, oxygen as well as limited nitrogen and potassium. Calculated from the XPS spectrum, the C : O : N : K atomic ratios in the CNDs are 41.4 : 15.4 : 1.1 : 1, respectively. In detail, the C_{1s} spectrum (Fig. 2b) shows three peaks at 283.0, 284.4 and 286.8 eV, which are attributed to the C–C, C–O and C=O/C=N, respectively. The O_{1s} spectrum exhibits two peaks at 531.0 and

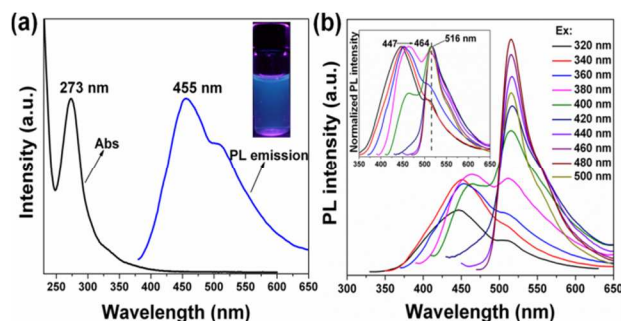


Fig. 3 (a) UV-Vis absorption and PL emission ($\lambda_{\text{ex}} = 360$ nm) spectrum, (b) the photoluminescent spectra of the CNDs at different excitation wavelengths as indicated.

533.7 eV, which are ascribed to the C=O and C-OH/C-O-C, respectively.^{22-24,31} Moreover, the N_{1s} and K_{2s} spectra are displayed in Electronic Supplementary Information (ESI, Fig. S1). The FTIR spectrum exhibits characteristic absorption bands of O-H, C-H, C=O, C=C, C-N, and C-O at 3430, 2931, 1698, 1631, 1517 and 1043 cm^{-1} , respectively. These observations clearly indicate that the CNDs are functionalized with carbonyl, carboxyl, hydroxyl, epoxy groups and amino group.^{32,33} The presence of these functional groups imparts excellent solubility in water without further chemical modification, which suggests that the obtained CNDs are most suitable for biological applications.

The absorption spectrum of the CNDs solution is shown in Fig. 3a, a distinct absorption peak at 273 nm, which can be attributed to the $\pi-\pi^*$ transition of nanocarbon.³⁴ The CNDs solution presents 455 nm PL emission peak when exciting at 365 nm wavelength, which is corresponding to the blue photoluminescent image (inset of Fig. 3a). To further investigate the photoluminescent properties of the as-prepared CNDs, we carried out a detailed PL study with different excitation wavelengths. As shown in Fig. 3b, when excitation wavelengths ranging from 320 to 500 nm, the PL emission spectra show unusual emission peaks, which are very different from the PL emission of other research reports.^{35,36} When the excitation wavelength ranges from 320 to 400 nm, the PL emission spectra show two peaks. The first emission peaks shift from 447 to 464 nm, presenting acquainted excitation-dependent PL behavior of the CNDs, which can probably be attributed to the presence of different particle sizes and the distribution of the different surface emission traps of the CNDs. Interestingly, the intensity of the second PL emission peaks, which locate at the position of about 516 nm, gradually increased with the red-shift of the excitation wavelength. When the excitation wavelength ranges from 420 to 500 nm, the emission spectra show only one peak around 516 nm, which is characteristic of the Mn(II) internal ${}^4T_1-{}^6A_1$ transition. Comparing to the emission peak reported previously at 585 nm,³⁷⁻³⁹ this about 69 nm blue-shift appears to be caused by the smaller size of the particles.⁴⁰ It is common knowledge that tea is rich in Mn element, and the CNDs are indeed demonstrated through plasma ICP-MS element analysis with the Mn content of 0.046%. It should be noted that the Mn element does not appear in the XPS spectrum just because of the minute amounts of Mn present. What is not expected is that the PLQY is as high as 6.8%, which is comparable with that of the CNDs previously reported.^{41, 42} Moreover, the Raman spectrum was not collected just because of the strong PL interference excited under wide wavelength.²⁵

The photostability of the CNDs have been also investigated. The PL intensity has almost no change when the CNDs were dissolved in DI water, upon exposure of daylight and xenon lamp with high intensity UV light for 6 hours, respectively (as shown in Fig. S2-a). The PL intensity hardly changed, demonstrating that the CNDs solution reveals fairly good photostability. Likewise, when the CNDs were dissolved in 0.1 mol/L NaCl solution, the CNDs also showed fairly good photostability (Fig. S2-b). Additionally, a negative charge (zeta potential = -33.1 mV, Fig. S3) was observed on the surfaces of the CNDs, which confirms the electrostatic stabilization of the CNDs aqueous solution.⁴³ The PL decay profile obtained from 455 nm emission at 360 nm excitation wavelength (Fig. S4) shows treble exponential decay kinetics. The parameters generated from iterative reconvolution of the decay with the instrument response function (IRF) are listed in the inset of Fig. S4. The average lifetime was calculated to be 4.36 ns, and the lifetime in the magnitude of nanosecond suggests that the synthesized CNDs are most suitable for optoelectronic and biological applications.^{44, 45} Furthermore, the PL decay profile obtained from 516 nm emission at 360 nm excitation wavelength was shown in the Fig. S5, the decay lifetime is about 0.78 ms, which is corresponding to the Mn(II) decay lifetime.^{46,47}

The feasibility of using this photoluminescent CNDs solution for detecting Hg^{2+} was investigated in Phosphate Buffered Solution (PBS, pH=7.0). It is seen that the CNDs solution in the absence of Hg^{2+} exhibits a strong fluorescence (Fig. 4a, curve A). In contrast, the presence of Hg^{2+} leads to an obvious PL intensity decrease (Fig. 4a, curve B), indicating that Hg^{2+} can effectively quench the photoluminescence of CNDs. This observation can be attributed to that the Hg^{2+} can quench the photoluminescence of CNDs via electron or energy transfer.⁴⁸⁻⁵⁰ Furthermore, the PLQY of CNDs is dropped to 3.5 % after addition of 100 μM Hg^{2+} . For sensitivity study, different

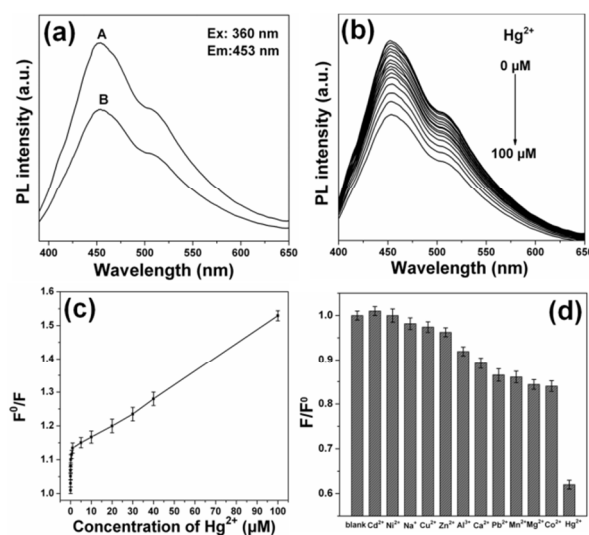


Fig. 4 (a) PL emission spectra of the CNDs dispersion in the absence (curve A) and presence (curve B) of Hg^{2+} ions, (b) PL spectra of CNDs dispersion in the presence of different Hg^{2+} concentrations (from top to bottom: 0, 0.0001, 0.001, 0.005, 0.01, 0.05, 0.1, 0.5, 1, 5, 10, 20, 30, 40, 50 and 100 μM), (c) the dependence of F^0/F on the concentrations of Hg^{2+} ions within the range of 0-100 μM , (d) the dependence of F/F^0 with the blank and solutions containing different metal ions (excitation at 360 nm, $[\text{ions}]=100$ μM).

concentrations of Hg^{2+} ranging from 1 nM to 100 μM were investigated. Fig. 4b shows the PL spectra of CNDs dispersion in the presence of different Hg^{2+} concentrations, revealing that the CNDs solution is sensitive to Hg^{2+} concentration and the PL intensity decreases with the increase of Hg^{2+} concentration. The detection limit is estimated to be 1 nM, which exhibits superior sensitivity than previously reported sensing systems (as shown in Table S1).⁵⁰⁻⁵² The detection limits also have been investigated when the PBS detection system was changed to real water system (lake water, or tap-water). In this real water system, the interference factor is significant, such as ions, bacteria, et al.. The lake water (the Yellow River, China) samples were filtered and then centrifuged at 15000 rpm for 30 min. The resultant water samples were spiked with Hg^{2+} at different concentration levels and then analyzed with the proposed method. The analysis results indicate that the detection limits can reach up to 700 nM and 200 nM for lake water system and tap-water system, respectively (as shown in Fig. S6). That is, in spite of the interference from numerous minerals and organics existing in the real water, the CNDs-based “sensor” can still distinguish between fresh real water and that spiked with Hg^{2+} .

The photoluminescence quenching was best described by the Stern–Volmer equation,⁵³

$$\frac{F^0}{F} = 1 + K_{SV}[Q],$$

where F and F^0 are the PL intensity of the CNDs solution in the presence and absence of Hg^{2+} , respectively. $[Q]$ is the concentration of the quencher (i.e., Hg^{2+}), and K_{SV} is the Stern–Volmer constant. The Stern–Volmer plot shown in Fig. 4c does not fit a conventional linear Stern–Volmer equation, indicating both dynamic and static quenching processes occur in this sensor system.^{54,55}

To evaluate the selectivity of this sensing system, we examined the PL intensity changes in the presence of representative metal ions under the same conditions (Fig. 4d). It is seen that a much lower PL intensity was observed for CNDs upon addition of Hg^{2+} . Moreover, the addition of Co^{2+} , Mn^{2+} , Ca^{2+} , Al^{3+} , [ions] = 100 μM) into CNDs- Hg^{2+} mixture gives slight effect on the detection of Hg^{2+} (Fig. S7). All these observations indicate that the sensing platform exhibits high selectivity for Hg^{2+} detection. The outstanding selectivity and specificity can be probably attributed to the chemical properties of Hg^{2+} which has a strong affinity for the carboxylic group on the CNDs surface than other metal ions. These above observations imply that the CNDs solution can be used as Hg^{2+} sensor and, upon further development, has potential for practical Hg^{2+} detection.

The possible application of obtained CNDs as cell-imaging agents was explored. The biocompatibility of CNDs was evaluated using human sarcoma cell (S180) lines and human hepatocyte (L02) lines through MTT assay. As shown in Fig. 5a, the obtained CNDs do not impose any significant toxicity to cells and are tolerable even at high dose (960 mg/mL), hence it is safe for *in vitro* and *in vivo* applications. Having established the biocompatibility, we performed *in vitro* cellular uptake experiments in S180 cells. As shown in Fig. 5b, the S180 cells incubated with CNDs in the medium presented bright, while showing blue and green colours upon excitation at 364 and 488 nm, respectively, by using a laser scanning confocal microscopy

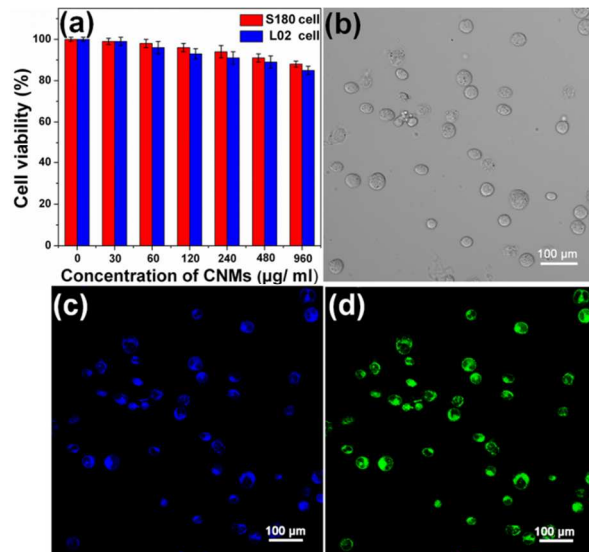


Fig. 5 (a) Cell viability by MTT assay, (b) S180 cells under bright field, (c) S180 cells under bright field, (d) S180 cells under bright field.

(Fig. 5c-d), which is corresponding to the above PL property. Obviously, the bright green luminescence of CNDs in the cell membrane and cell cytoplasm regions was observed, while the image is dark in the cell nucleus, which demonstrates that the CNDs are able to label the cell membrane and cell cytoplasm. Such observations indicate that the CNDs from green tea serve as a potential, ideal probe for cell imaging.

Conclusion

In summary, water-soluble, manganiferous, photoluminescent carbonaceous nanomaterials have been discovered in a cup of tea. Such CNDs exhibit small particles, amorphous structure and novel photoluminescent properties. The component and surface state investigated by FTIR and XPS demonstrated the excellent water solubility of the CNDs. Moreover, these CNDs can serve as an efficient photoluminescent sensing probe for sensitive, selective detection of Hg^{2+} and cell-imaging. These observations are interesting and important because they provide a very simple, immediate and low cost route toward environmentally friendly production of photoluminescent carbon nanomaterials for sensing, bioimaging, optical imaging and a wide range of other applications.

Acknowledgement

This study is supported by Chongqing Natural Science Foundation (cstc2013jcyjA20023), Scientific and Technological Research Program of Chongqing Municipal Education Commission (KJ1401111).

Notes and references

- ^a College of Chemistry and Materials Engineering, Anhui Science and Technology University, Fengyang 233100, People's Republic of China.
- ^b Research Institute for New Materials Technology, Chongqing University of Arts and Sciences, Chongqing 402160, People's Republic of China.
- ^c Department of Tea science, Xinyang College of Agriculture and Forestry, Xinyang 464000, People's Republic of China.
- [†] These authors contributed equally to this work.

* Corresponding author. Tel.: +86 18203053507; fax: +86 73184618071.

E-mail address: liubitao007@163.com (Bitao Liu).

- [1] H. W. Kroto, J. R. Heath, S. C. O'Brien, R. F. Curl and R. E. Smalley, *Nature*, 1985, 318, 162.
- [2] H. L. Li, J. F. Zhai, and X. P. Sun, *Nanoscale*, 2011, 3, 2155.
- [3] Z. Yang, Z. Cao, H. Sun, and Y. Li, *Adv. Mater.*, 2008, 20, 2201.
- [4] K. S. Novoselov, A. K. Geim, S. V. Morozov, D. Jiang, Y. Zhang, S. V. Dubonos, I. V. Grigorieva and A. A. Firsov, *Nature*, 2004, 306, 666.
- [5] D. R. Larson, W. R. Zipfel, R. M. Williams, S. W. Clark, M. P. Bruchez, F. W. Wise and W. W. Webb, *Science*, 2003, 300, 1434.
- [6] S. Liu, J. Q. Tian, L. Wang, Y. L. Luo, J. F. Zhai and X. P. Sun, *J. Mater. Chem.*, 2011, 21, 11726.
- [7] X. Y. Qin, A. M. Asiri, K. A. Alamry, A. O. Al-Youbi, X. P. Sun, *Electrochim. Acta*, 2013, 95, 260.
- [8] X. Y. Qin, W. B. Lu, A. M. Asiri, A. O. Al-Youbi, X. P. Sun, *Sens. Actuator B*, 2013, 184, 156.
- [9] W. B. Lu, X. Y. Qin, A. M. Asiri, A. O. Al-Youbi, X. P. Sun, *J. Nanaopar. Res.*, 2013, 15, 1344.
- [10] H. L. Li, J. F. Zhai, J. Q. Tian, Y. L. Luo, X. P. Sun, *Biosens. Bioelectron.*, 2011, 26, 4656.
- [11] J. M. Wei, J. M. Shen, X. Zhang, S.K. Guo, J.Q. Pan, X.G. Hou, H. B. Zhang, L. Wang, B. X. Feng, *RSC Adv.*, 2013, 3, 13119.
- [12] J. C. G. Esteves da Silva and H. M. R. Goncalves, *Trends Anal. Chem.*, 2011, 30, 1327.
- [13] H. X. Zhao, L. Q. Liu, Z. D. Liu, Y. Wang, X. J. Zhao and C. Z. Huang, *Chem. Commun.*, 2011, 47, 2604.
- [14] C. X. Guo, H. B. Yang, Z. M. Sheng, Z. S. Lu, Q. L. Song and C. M. Li, *Angew. Chem., Int. Ed.*, 2010, 122, 3078.
- [15] X. Y. Qin, W. B. Lu, A. M. Asiri, A. O. Al-Youbi, and X. P. Sun, *Catal. Sci. & Technol.*, 2013, 3, 1027.
- [16] X. Y. Qin, S. Liu, W. B. Lu, H. Y. Li, G. H. Chang, Y. W. Zhang, J. Q. Tian, Y. L. Luo, A. M. Asiri, A. O. Al-Youbi, and X. P. Sun, *Catal. Sci. Technol.*, 2012, 2, 711.
- [17] X. Y. Qin, W. B. Lu, G. H. Chang, Y. L. Luo, A. M. Asiri, A. O. Al-Youbi, X. P. Sun, *Gold Bull.*, 2012, 45, 61.
- [18] A. B. Bourlino, A. Stassinopoulos, D. Anglos, R. Zboril, M. Karakassides and E. P. Giannelis, *Small*, 2008, 4, 455.
- [19] S. Liu, J. Q. Tian, L. Wang, Y. L. Luo and X. P. Sun, *RSC Adv.*, 2012, 2, 411.
- [20] S. Liu, L. Wang, J. Q. Tian, J. F. Zhai, Y. L. Luo, W. B. Lu and X. P. Sun, *RSC Adv.*, 2011, 1, 951.
- [21] L. Zheng, Y. Chi, Y. Dong, J. Lin and B. Wang, *J. Am. Chem. Soc.*, 2009, 131, 4564.
- [22] X. Xu, R. Ray, Y. Gu, H. J. Ploehn, L. Gearheart, K. Raker and W. A. Scrivens, *J. Am. Chem. Soc.*, 2004, 126, 12736.
- [23] H. Peng, J. Travas-Sejdic, *Chem. Mater.*, 2009, 21, 5563.
- [24] S. Sahu, B. Behera, T. K. Maiti, S. Mohapatra, *Chem. Commun.*, 2012, 48, 8835.
- [25] C. Zhu, J. Zhai, S. Dong, *Chem. Commun.*, 2012, 48, 9367.
- [26] M. Hara, T. Yoshida, A. Takagaki, T. Tsuyoshi, J. N. Kondo, S. Hayashi, K. Domen, *Angew. Chem. Int. Ed.*, 2004, 43, 2955.
- [27] N. Tsubouchi, K. Xu, Y. Ohtsuka, *Energy Fuels*, 2003, 17, 1119.
- [28] D. Bibekananda, K. Niranjana, *RSC Adv.*, 2013, 3, 8286.
- [29] H. Ming, Z. Ma, Y. Liu, K. M. Pan, H. Yu, F. Wang and Z. H. Kang, *Dalton Trans.*, 2012, 41, 9526.
- [30] H. P. Liu, T. Ye and C. D. Mao, *Angew. Chem., Int. Ed.*, 2007, 46, 6473.
- [31] W. W. Lei, D. Portehault, R. Dimova, M. Antonietti, *J. Am. Chem. Soc.*, 2011, 133, 7121.
- [32] Y.Q. Zhang, D.K. Ma., Y. Zhuang, X. Zhang, W. Chen, L. L. Hong, Q. X. Yan, K. Yu, S. M. Huang, *J. Mater. Chem.*, 2012, 22, 16714.
- [33] Z. Ma, H. Ming, H. Huang, Y. Liu, Z. H. Kang, *New J. Chem.*, 2012, 36, 861.
- [34] P. Yu, X. Wen, Y.R. Toh, J. Tang, *Nano Lett.*, 2012, 116, 25552.
- [35] H. T. Li, Z.H. Kang, Y. Liu and S-T Lee., *J. Mater. Chem.*, 2012, 22, 24230.
- [36] J. M. Wei, X. Zhang, Y. Z. Sheng, J. M. Shen, P. Huang, S. K. Guo, J. Q. Pan, B.T. Liu and B. X. Feng, *New J. Chem.*, 2014, 38, 906.
- [37] R. N. Bhargava, D. Gallagher and A. Nurmikko, *Phys. Rev. Lett.*, 1994, 72, 416.
- [38] A. Aboulaich, M. Geszke, L. Balan, J. Ghanbaja, G. Medjahdi, R. Schneider, *Inorg. Chem.*, 2010, 49, 10940.
- [39] H. Y. Chen, S. Maiti, and D. H. Son, *ACS Nano*, 2012, 6, 583.
- [40] M. A. Malik, P. O'Brien, N. Revaprasadu, *J. Mater. Chem.*, 2001, 11, 2382.
- [41] Y. P. Sun, X. Wang, F. S. Lu, L. Cao, M. J. Meziani, P. J. G. Luo, L. R. Gu and L. M. Veca, *J. Phys. Chem. C*, 2008, 112, 18295.
- [42] S. N. Baker and G. A. Baker, *Angew. Chem., Int. Ed.*, 2010, 49, 6726.
- [43] D. Li, M. B. Muller, S. Gilje, R. B. Kaner and G. G. Wallace, *Nat. Nanotechnol.*, 2008, 3, 101.
- [44] J. Peng, W. Gao, B. K. Gupta, Z. Liu, R. R. Aburto, L. Ge, L. Song, L. B. Alemany, X. Zhan, G. Gao, S. A. Vithayathil, B. A. Kaipparattu, A. A. Marti, T. Hayashi, J-J. Zhu, and P. M. Ajayan, *Nano Lett.*, 2012, 12, 844.
- [45] A. Aboulaich, M. Geszke, L. Balan, J. Ghanbaja, G. Medjahdi, R. I. Schneider, *Inorg. Chem.*, 2010, 49, 10940.
- [46] J. Zheng, X. Yuan, M. Ikezawa, P. Jing, X. Liu, Z. Zheng, X. Kong, J. Zhao, Y. Masumoto, *J. Phys. Chem. C*, 2009, 113, 16969.
- [47] H. Chakraborti, S. Sinaha, S. Ghosh and S. K. Pal, *Mater. Lett.*, 2013, 97, 78.
- [48] S. Liu, J. Tian, L. Wang, Y. Zhang, X. Qin X, Y. Luo, et al., *Adv. Mater.*, 2012, 24, 2037.
- [49] F. Pu, Z. Z. Huang, J. S. Ren, and X. G. Qu, *Anal. Chem.*, 2010, 82, 8211.
- [50] W. B. Lu, X. Y. Qin, S. Liu, G. H. Chang, Y. W. Zhang, Y. L. Luo, A. M. Asiri, A. O. Al-Youbi, and X. P. Sun, *Anal. Chem.*, 2012, 84, 5351.2037.
- [51] S. Liu, X. Y. Qin, J. Q. Tian, L. Wang, X. P. Sun, *Sens. Actuator B*, 2012, 171-172, 886.
- [52] L. Wang, J. Q. Tian, H. L. Li, Y. W. Zhang, X. P. Sun, *J. Fluoresc.* 2011, 21, 1049.
- [53] G. Liang, H. Liu, J. Zhang, J. J. Zhu, *Talanta*, 2010, 80, 2172.
- [54] Y. Chen, Z. Rosenzweig, *Anal. Chem.* 2002, 74, 5132.
- [55] Y. H. Chan, J. Chen, Q. Liu, S. E. Wark, D. H. Son, J. D. Batteas, *Anal. Chem.* 2010, 82, 3671.